A growing self-avoiding walk in three dimensions and its relation to percolation

R. Mark Bradley
Department of Physics, Colorado State University, Fort Collins, Colorado 80523

P. N. Strenski
IBM Thomas J. Watson Research Center, Yorktown Heights, New York 10598

Jean-Marc Debierre*
Department of Physics, Colorado State University, Fort Collins, Colorado 80523
(Received 6 February 1992)

We introduce a growing self-avoiding walk in three dimensions (3D) that can terminate only by returning to its point of origin. This "tricolor walk" depends on two parameters, p and q, and is a direct generalization of the smart kinetic walk to 3D. Our walk is closely related to percolation with three colors (black, white, and gray): the tricolor walk directly constructs a loop formed by the confluence of a black, a white, and a gray cluster. The parameters p and q are the fraction of sites colored black and white, respectively. We present numerical and analytical evidence that for $p=q=\frac{1}{3}$, the fractal dimension of the tricolor walk is exactly 2. For $p=q<\frac{1}{3}$, the walks undergo a percolation transition at $p\cong 0.2915$. Our Monte Carlo simulations strongly suggest that this transition is not in the same universality class as the usual percolation transition in 3D. The mean length of the finite walks χ is divergent throughout an extended region of the parameter space.

PACS number(s): 64.60.Ak, 36.20.Ey, 05.40.+j, 64.60.Fr

I. INTRODUCTION

The equilibrium behavior of long polymer chains in a good solvent has been the subject of much research over the past four decades and is now quite well understood [1]. Chains of this kind are commonly modeled as self-avoiding walks (SAW's). In most studies, the process of polymerization (if present at all) is so slow that it may be neglected on time scales characterizing chain fluctuations. Recently, however, there has been a great deal of interest in the opposite, far-from-equilibrium limit of rapid polymerization [2–10]. This interest has centered on the properties of growing SAW's. Although at first there were difficulties in finding growing walks that grow indefinitely and that are strictly self-avoiding [2,3], several such walks are now known in two dimensions (2D) [4–9]. The most extensively studied and simplest of these walks in the smart kinetic walk (SKW) [4–6]. The SKW on the hexagonal lattice depends on a single parameter p. At the critical point $p=\frac{1}{2}$, the walks have fractal dimension $D_{\mathrm{SKW}}=\frac{7}{4}$ [11]. A second indefinitely growing SAW, the diffusion-limited self-avoiding walk (DLSAW), was introduced by Bradley and Kung [7] and by Debierre and Turban [8] as a model of the diffusion-limited growth of a polymer chain in a dilute solution of monomers [12]. Their Monte Carlo studies in 2D yielded the fractal dimension $D_{\mathrm{DLSAW}}=1.29\pm 0.01$ [13]. Both of these results differ from the fractal dimension of the equilibrium SAW in its high-temperature phase [14], $D_{\mathrm{EQSAW}}=\frac{4}{3}$.

Growing SAW's in three dimensions (3D) have received much less attention, even though they are of greater physical interest. The kinetic growth walk does not grow indefinitely, and is believed to slowly cross over to a regime in which it has the same scaling behavior as the equilibrium SAW in 3D [15]. The SKW has not been simulated in 3D, since it has not been clear how to generalize the growth algorithm to dimensions d higher than 2. The algorithm used to generate the DLSAW is readily extended to $d>2$, on the other hand, and simulations of the model have been performed in three and four dimensions [7,10]. Finally, Lyklema introduced the growing self-avoiding trail (GSAT) and studied it in 2D and 3D by the Monte Carlo method [16]. Self-avoiding trails are walks which may revisit sites but not bonds, and so display a kind of partial self-avoidance.

In addition to being important in the theory of growing polymer chains, the study of the SKW in 2D is relevant to several other topics of current theoretical interest. The SKW on the hexagonal lattice has been shown to trace out the perimeter or "hull" of a percolation cluster [4], and so gives a method of directly constructing these perimeters [17]. This has greatly facilitated Monte Carlo studies of percolation hulls. For $p=\frac{1}{2}$, right and left turns are equally probable in the SKW on the hexagonal lattice, and the model can be mapped onto a certain self-attracting SAW at its collapse transition [18,19]. This correspondence has engendered considerable progress in the understanding of the 2D Θ point [18–20].

There are two ways in which the SKW can be generalized to 3D. Recently, we discussed one of the possible generalizations: the smart kinetic surface (SKS) [21,22]. The SKS is a growing self-avoiding surface which directly generates the hull of a percolation cluster in 3D. The SKS was employed in Refs. [21] and [22] to determine the scaling properties of 3D percolation hulls with much

greater precision than in previous studies.

In this paper we introduce a growing SAW in 3D, the tricolor walk. The tricolor walk is the second direct generalization of the SKW to three dimensions, and depends on two parameters, p and q. The tricolor walk is "smart"—it cannot self-trap—and yet it is readily simulated. An important special case of the model is the symmetric tricolor walk, in which all allowed moves for the walker are equally weighted and $p=q=\frac{1}{3}$. Our extensive Monte Carlo simulations of the symmetric tricolor walk strongly suggest that its fractal dimension is 2. We show that the symmetric tricolor walk is equivalent to a self-attracting SAW in equilibrium, and then use this equivalence to argue that the fractal dimension of the symmetric tricolor walk must be exactly 2. As a by-product, we obtain the exact Θ temperature for a self-attracting SAW in 3D.

Polychromatic percolation with n colors is a generalization of percolation in which each lattice site can take on one of n states or "colors" [23,24]. It has been suggested that polychromatic percolation may be applied to such diverse materials as sodium-ammonia mixtures [25,26], charge transfer salts [26], and magnets with an inverse spinel structure [24,27]. In the present work, we will demonstrate that the tricolor walk constructs a loop formed by the confluence of a black, a white, and a gray cluster in polychromatic percolation with three colors. Thus, just as in the case of the SKW on the 2D hexagonal lattice, there are close connections with percolation and self-attracting SAW's.

We shall also study asymmetric tricolor walks with $p=q<\frac{1}{3}$. These walks undergo a percolation transition as the parameter p is reduced below a threshold value $p=p_1$: there are infinite walks for $p_1<p<\frac{1}{3}$, but not for $p<p_1$. Surprisingly, some of the critical exponents describing this transition seem to be the same as in regular percolation in 3D, but others are different. The mean length of the closed walks χ is divergent for $p_1<p\leq\frac{1}{3}$. In contrast, in regular percolation χ is finite for all values of p except the threshold value p_c.

The paper is organized as follows: In Sec. II the tricolor walk is defined and its relation to trichromatic percolation is established. We describe our Monte Carlo and analytical results for the symmetric tricolor walk in Sec. III. The asymmetric tricolor walk is considered in Sec. IV. The paper closes with our conclusions in Sec. V.

II. THE TRICOLOR WALK

The growth of the tricolor walk is analogous to that of the SKW in 2D. We will therefore briefly recall the growth algorithm for the SKW and show that the SKW traces out the hull of a percolation cluster. We will only consider the growth of the SKW on the hexagonal lattice, since this is the simplest case and is the closest analog to the tricolor walk. For further details and generalizations to different lattices, we refer the reader to Refs. [4] and [17].

Consider site percolation on the triangular lattice. A hull of a percolation cluster is made up of bonds on the Wigner-Seitz (WS) lattice that cut bonds joining unoccupied and occupied sites. A hull is a connected set of these bonds on the dual lattice. A given cluster has one external hull, and may have one or more internal hulls.

The SKW is a kinetic self-avoiding walk on the WS lattice, which is hexagonal. At the outset, the occupancy of sites on the original lattice is unspecified. The SKW begins by traversing a given bond on the WS lattice. The site on the original lattice to the right of the step is occupied, while the site to the left is unoccupied. The first step in the walk points toward a site on the original lattice. This site is now specified to be occupied with probability p or unoccupied with probability $1-p$. If the site is occupied, the walk turns left; otherwise, it turns right (Fig. 1). The walk now continues in this way. If at any time the last step of the walk points toward a site whose occupancy has already been specified, it turns left if this site is occupied and right if it is unoccupied. The walk ends when it returns to its point of origin. Clearly, the SKW traces out a hull of a site percolation cluster on the triangular lattice. We will call the SKW with $p=\frac{1}{2}$ "unbiased" since allowed moves are equally weighted.

The hulls in site percolation on the triangular lattice are particularly simple because the WS lattice is threefold coordinated, and this is the lowest coordination number a 2D lattice can have. In addition, each site on the WS lattice either belongs to two bonds in a hull, or to none. This is in contrast to the situation for site percolation on the square lattice. In that case, a site on the WS lattice can be shared by zero, two, or four bonds in hulls. As a result, it is possible to define two different hulls for site percolation on the square lattice [28]. One of these hulls has sites in the dual lattice that are shared by four hull bonds, while the other does not. This difference is significant, because these two hulls have different fractal dimensions [28]. Site percolation on the triangular lattice is appealingly simple because there is only one possible definition of the hull.

The SKW is called "smart" because it can only ter-

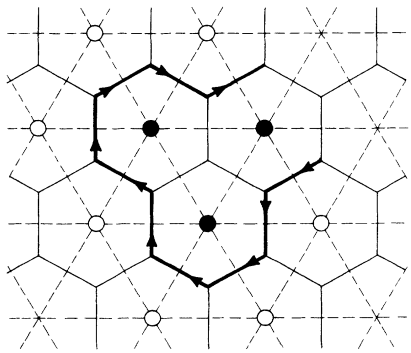

FIG. 1. SKW on the hexagonal lattice. The original triangular lattice is shown with dashed lines, while the hexagonal Wigner-Seitz lattice is shown with solid lines. Solid and open circles at the vertices of the original lattice indicate sites which have been specified to be occupied or unoccupied, respectively. The SKW itself is shown with bold directed lines. This SKW occurs with probability $p^2(1-p)^6$.

minate by returning to its point of origin—it cannot enter a cul-de-sac from which there is no escape. The SKW is also strictly self-avoiding. Finally, note that these two observations can be combined into the single assertion that each site in the completed walk belongs to precisely two occupied bonds.

We now generalize these ideas to 3D. We must first recall the definition of polychromatic site percolation with three colors, or "trichromatic percolation" [23,24]. In trichromatic percolation, each site is colored black with probability p, white with probability q, and gray with probability $r=1-p-q$. Adjacent sites belong to the same cluster if they have the same color. Ordinary two-color site percolation is recovered if either p, q, or r is zero.

A percolation hull is an interface between regions of two different colors. Two nontrivial types of interfaces can be defined for 3D trichromatic percolation. A connected surface of a cluster will be called a "hull." A hull separates a cluster from a set of adjacent sites which bear different colors than the sites in the cluster itself. In 3D, trichromatic percolation hulls have the same properties as the hulls in ordinary site percolation, and the latter have been considered in detail elsewhere [21,22]. A region where all three colors meet will be called a "tricord." Tricords have not previously been considered, and will be studied in the present paper. The tricolor walk will be defined so that it constructs a tricord for trichromatic percolation, just as the SKW on the hexagonal lattice produces a hull.

We have elected to study trichromatic site percolation on the body-centered cubic (bcc) lattice. In the problem we shall consider, both nearest-neighbor (NN) and next-nearest-neighbor (NNN) sites of the same color are taken to be in the same cluster. The percolation threshold p_c for two-color percolation on the bcc lattice with both NN and NNN bonds has not yet been estimated. However, it must be less than the threshold for the two-color site problem with NN bonds only, $p_c'=0.2460\pm0.0003$ [21,22], and so $p_c<\frac{1}{3}$. Thus, in our problem, there is a region in the (p,q) plane in which all three colors percolate simultaneously: the three colors percolate provided that $p\geq p_c$, $q\geq p_c$, and $r=1-p-q\geq p_c$. In particular, the three colors percolate for $p=q=\frac{1}{3}$. We therefore may expect infinite tricords to occur for a range of p and q values close to $\frac{1}{3}$. Note, however, that the mere occurrence of infinite clusters of all three colors does not guarantee the existence of an infinite tricord.

The WS cell of the bcc lattice is a truncated octahedron, which is a regular polyhedron with eight hexagonal faces and six square faces. The WS lattice is constructed by packing truncated octahedra to fill space and is fourfold coordinated (Fig. 2). A site of the original lattice resides at the center of each WS cell. Note that each bond in the WS lattice belongs to three WS cells. Accordingly, we can label a particular bond by the unordered triplet (S_1,S_2,S_3), where sites S_1, S_2,and S_3 are the sites at the centers of the three WS cells that contain the bond. We will also say that the sites S_1, S_2, and S_3 are adjacent to the bond (S_1,S_2,S_3).

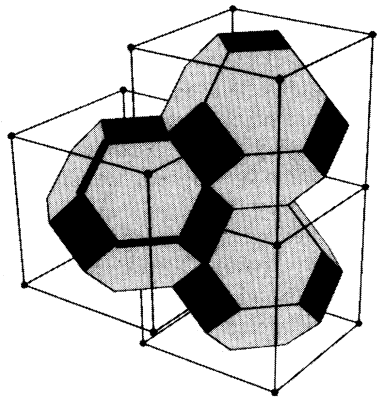

FIG. 2. Wigner-Seitz lattice for the bcc lattice. The sites of the bcc lattice (solid circles) form two interpenetrating simple cubic lattices. The Wigner-Seitz lattice is a space-filling packing of truncated octahedra (shaded solids). A site of the bcc lattice resides at the center of each truncated octahedron. An example of a SKW that cannot be generated by the tricolor walk is shown using bold lines.

We can now define the tricord more precisely for trichromatic site percolation on the bcc lattice. A bond (S_1,S_2,S_3) in the WS lattice will be called a tricord bond if the adjacent sites S_1,S_2, and S_3 have different colors. A tricord is defined to be a connected set of tricord bonds. Because we consider NN and NNN sites of the same color to belong to the same cluster, all the black sites adjacent to the tricord belong to the same cluster. The same is true for all the white and all the gray sites adjacent to the tricord. A tricord is therefore a loop formed by the confluence of a black, a white, and a gray cluster. Infinite tricords can exist only if there is at least one infinite cluster of each of the three colors.

The tricords in trichromatic site percolation on the bcc lattice are especially simple for two reasons. First, the WS lattice is fourfold coordinated, and this is the lowest coordination number a 3D lattice can have. Secondly, each site in the WS lattice either does not belong to a tricord, or is shared by exactly two bonds in a tricord. Each tricord is therefore a closed loop of bonds in the WS lattice. This is much simpler than the situation for the simple cubic lattice. Sites in the WS lattice of the simple cubic lattice can be shared by 0, 2, 3, 4, 5, or 6 bonds in tricords [29], and thus there is more than one possible definition of the tricord, just as more than one hull can be defined for site percolation on the square lattice [28].

The tricolor walk is a random walk on the WS lattice. Initially all sites in the original lattice are uncolored, and the bonds in the WS lattice are all unoccupied. At the first time step, the walk traverses a bond labeled (S_1^0,S_2^0,S_3^0). Sites S_1^0,S_2^0, and S_3^0 are now colored black, white, and gray, respectively. Now consider the growth of the walk an arbitrary length of time later, and suppose that the walk has just traveled along the bond (S_1,S_2,S_3). We may assume that sites S_1, S_2, and S_3 are colored black, white, and gray, respectively. The site on

the WS lattice which has just been occupied belongs to four WS cells. Sites S_1, S_2,and S_3 lie at the centers of three of these cells. Let site S_4—the "target site"—be the site at the center of the fourth WS cell. If S_4 is uncolored, it is colored black with probability p, white with probability q, and gray with probability $r=1-p-q$. If the target site is already colored, its coloring is left unchanged. The next step of the walk is now made. If S_4 is black, the walk traverses the bond (S_4,S_2,S_3). If S_4 is white, the walk travels along the bond (S_1,S_4,S_3). Finally, if S_4 is gray, the bond (S_1,S_2,S_4) is occupied. In each case, the newly occupied bond belongs to the tricord. The walk terminates if it returns to its point of origin. Walks with $p=q=r=\frac{1}{3}$ will be called symmetric, while walks with different values of p, q, and r will be referred to as asymmetric.

It is clear that the tricolor walk traces out a tricord for trichromatic site percolation on the bcc lattice with both NN and NNN bonds. In addition, the walk is both strictly self-avoiding and smart because each site in the completed walk belongs to precisely two occupied bonds. The tricolor walk is therefore a natural generalization of the SKW to 3D.

The tricolor walk is not the only possible generalization of the 2D SKW to 3D. We have defined the SKW on the hexagonal lattice in the same way as Weinrib and Trugman [4]. However, the unbiased SKW on the hexagonal lattice can be defined in a different but equivalent fashion [5,6]. In this alternative approach, a move is called "smart" if the new site has not previously been visited and if after making the move the walker can still return to its point of origin without violating the self-avoidance constraint. At a given time step, all smart moves are weighted equally. This alternative definition is not restricted to the hexagonal lattice, and can be equally well applied in 3D. In particular, it can be applied to the WS lattice for the bcc lattice. The resulting SKW differs from the symmetric tricolor walk, since some SKW configurations with nonzero weight cannot occur in the tricolor walk (Fig. 2). However, it is by no means obvious how to carry out simulations of the SKW in 3D, while the tricolor walk is readily simulated.

III. SYMMETRIC TRICOLOR WALK

We will begin our study of the symmetric tricolor walk by attempting to anticipate its behavior, based on the analogy with the SKW on the hexagonal lattice. The resulting conjectures on the behavior of the symmetric tricolor walk will then be tested by Monte Carlo simulations.

First, consider the SKW for $p=\frac{1}{2}$. For this value of p, the colors black and white are equally probable. The walks generated are scale invariant [4] with a fractal dimension of $\frac{7}{4}$ [11], and the probability $P(N)$ that a loop of length N is formed has the power-law scaling behavior $P(N)\sim N^{-\tau'+1}$ for large N. The exact value of the critical exponent τ' is $\frac{15}{7}$ [30]. Thus $p=\frac{1}{2}$ is a critical point for the SKW. Now consider the symmetric tricolor walk. When $p=q=r=\frac{1}{3}$, the three colors black, white, and gray are equally probable. By analogy with the behavior of the SKW, we expect $p=q=\frac{1}{3}$ to be a critical point for the tricolor walk. Accordingly, we expect that the walks will be scale invariant with a fractal dimension D_3, and that $P(N)$ will decay as $N^{-\tau_3+1}$ for large N. The critical exponents D_3 and τ_3 will be determined below.

A. Monte Carlo results

We first performed Monte Carlo simulations of the symmetric tricolor walk. Each walk either closed or grew to the maximum permitted length of $N_{\max}=2^{20}=1\,048\,576$ steps. A total of 10 000 walks were constructed, which required a total of roughly 60 CPU hours on an IBM RISC System/6000 model 540. A typical walk of length 10 000 is shown in Fig. 3.

Of the 10 000 walks generated, a total of 6269 had not closed when they reached length $N_{\max}$. For these open chains, we computed the average square distance $\langle R^2(\Delta)\rangle$ between sites Δ steps apart for $\Delta=1,2,2^2,\ldots,2^{20}$. For each value of Δ, we averaged over each pair of points separated by Δ steps within a chain, and then averaged over all the open chains. A log-log plot of $\langle R^2(\Delta)\rangle$ versus Δ (Fig. 4) reveals a linear region three decades wide, and so strongly supports our identification of $p=q=\frac{1}{3}$ as a critical point for the tricolor walk. A least-squares fit to all but the first four points gives the estimate $D_3=2.029\pm0.003$ for the fractal dimension. The error quoted here is the standard deviation obtained by a least-squares fit, and does not take into account any systematic errors present. To obtain a more reliable estimate of D_3, we computed the finite-size estimator

$$D_e(\Delta)\equiv \ln 4[\ln\langle R^2(\Delta)\rangle-\ln\langle R^2(\Delta/2)\rangle]^{-1} \tag{3.1}$$

for $\Delta=2,2^2,\ldots,2^{20}$. For large Δ, the estimator $D_e(\Delta)$ converges to the fractal dimension D_3. Our results are

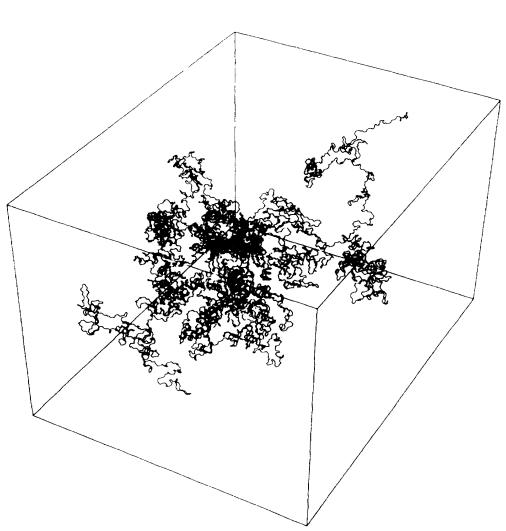

FIG. 3. A typical open symmetric tricolor walk of length 10 000. The box is shown to give an impression of depth; its sides are parallel to the x, y, and z axes.

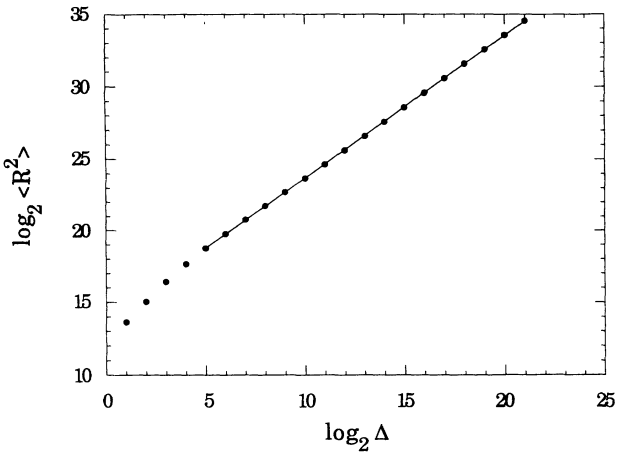

FIG. 4. Log-log plot of the mean square distance $\langle R^2 \rangle$ between two sites separated by Δ steps as a function of Δ for the open symmetric walks. The straight line is a linear least-squares fit to the data points for $\Delta \geq 32$. This fit gives the estimate $D_3 = 2.029 \pm 0.003$ for the fractal dimension of the symmetric walks.

shown in Fig. 5. $D_e(\Delta)$ overshoots the value 2 and then decreases towards it. Note that the standard deviation of the data increases with Δ because there are fewer pairs of points separated by Δ steps when Δ is large. Based on these results, we think that it is likely that the asymptotic value of D_3 is 2. As we shall see in Sec. III B, there are also good theoretical reasons for believing that this is the exact fractal dimension.

Now consider the closed loops. The mean square radius of gyration of a loop of length N is defined to be

$$\langle R^2(N) \rangle \equiv \frac{1}{N^2} \left\langle \sum_{i=1}^{N} \sum_{j=1}^{N} (\mathbf{r}_i - \mathbf{r}_j)^2 \right\rangle , \tag{3.2}$$

where $\mathbf{r}_i$ is the position of the walk after i steps. Because there were a comparatively small number of large loops, the data were binned as follows. A walk of length N belongs to the ith bin if $n_i \leq N < n_{i+1}$, where $n_i = 2^{i+1}$. We computed the average length N_i and the average radius of gyration R_i of the loops in the ith bin for each i. A log-log plot of our data is shown in Fig. 6. A least-squares fit for $i \geq 2$ yields the estimate $D_3 = 2.04 \pm 0.02$ for the fractal dimension. Once again, the error given is the value of the standard deviation and does not take into account the possibility that a systematic error is present. Indeed, based on our analysis of the open chains, we expect that a gradual decrease in the apparent value of the fractal dimension would occur if still larger chains were constructed [31]. The data for the closed loops are therefore consistent with the conjectured value $D_3 = 2$.

According to the analogy with the SKW in 2D, the probability $P(N)$ that a walk closes after exactly N steps should scale as $N^{-\tau_3+1}$ for sufficiently large N. Let $P_i \equiv [\sum_{N=n_i}^{n_{i+1}-1} P(N)]/(n_{i+1} - n_i)$ denote the probability that a closed walk lies in the ith bin divided by the length of the bin. We then have $P_i \sim N_i^{-\tau_3+1}$. Figure 7 is a log-log plot of our data for P_i versus N_i. A linear fit for $i \geq 3$ gives the estimate $\tau_3 = 2.49 \pm 0.1$ for the exponent τ_3. In Sec. III B we argue that the exact value of τ_3 is $\frac{5}{2}$, and this is in excellent agreement with our Monte Carlo result.

The fraction $F(N)$ of the walks which have not closed after N steps should scale as

$$F(N) \cong A + BN^{-\tau_3+2} \tag{3.3}$$

for $N \gg 1$. Here A is the probability that a given walk never closes. We used the conjectured exact result $\tau_3 = \frac{5}{2}$ to compute the constants A and B appearing in the scaling form (3.3). A linear fit of $F(N)$ as a function of $1/\sqrt{N}$ for $N \geq 12$ gave $A = 0.628 \pm 0.001$ and $B = 1.04 \pm 0.01$ (Fig. 8). On the 2D Manhattan lattice, the probability that an unbiased SKW exceeds length N asymptotes to zero as $N \to \infty$ [32], and we believe that the same is true for unbiased SKW's on arbitrary 2D lat-

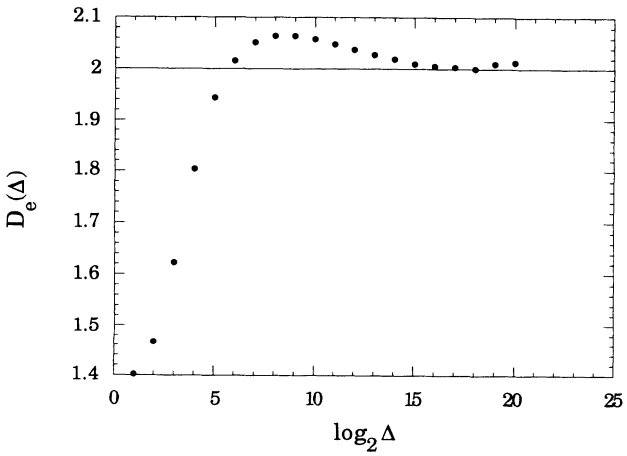

FIG. 5. The finite-size estimator $D_e(\Delta)$ for the fractal dimension of the open symmetric walks as a function of $\log_2 \Delta$. $D_e(\Delta)$ appears to converge to 2 as Δ grows large.

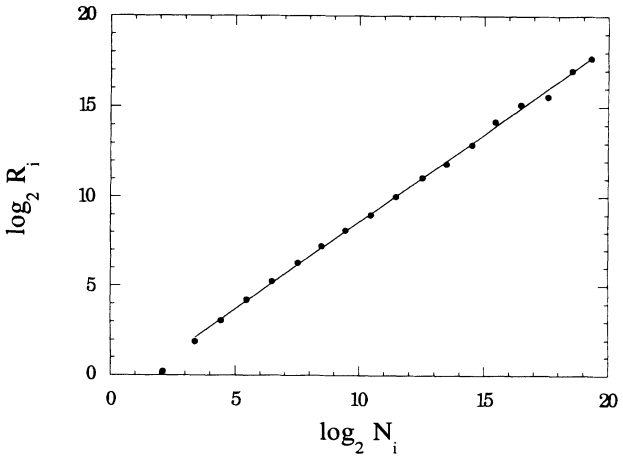

FIG. 6. Log-log plot of the mean radius of gyration R_i vs the mean length N_i for the closed symmetric walks in the ith bin. A linear fit to all but the first data point gives $D_3 = 2.04 \pm 0.02$.

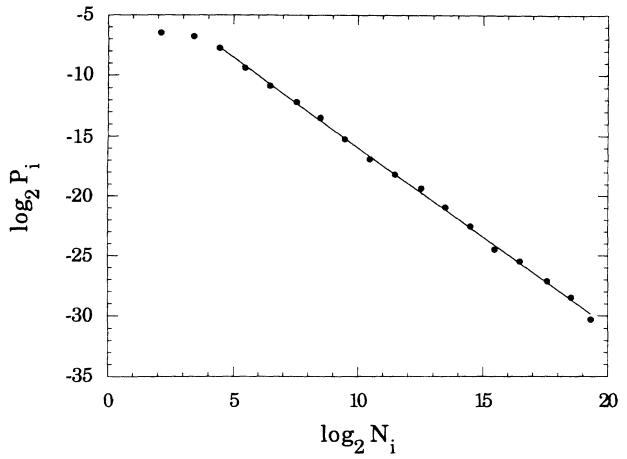

FIG. 7. Log-log plot of P_i as a function of N_i for the symmetric walks in the ith bin. The solid line is a linear fit to the data points for $i \geq 3$, and yields the estimate $\tau_3 = 2.49 \pm 0.01$.

tices. At first glance, therefore, it is surprising that A is nonzero for the tricolor walk. This difference between the SKW in 2D and the tricolor walk is readily understood, however. In 3D, there is a nonzero probability that a pure random walk never returns to its point of origin [33]. Since the tricolor walk is self-avoiding, it is less likely to return to its starting point than a pure random walk, and there is a nonzero probability that it never closes. We therefore expect the tricolor walk to have a nonzero value of A, and this expectation is borne out by our simulations. This argument cannot be applied to the SKW on a 2D lattice, because in 2D a random walk always returns to its starting point after a sufficient length of time [33].

B. Equivalent equilibrium polymer problem

We now show that the symmetric tricolor walk is equivalent to a self-attracting self-avoiding loop (SASAL)

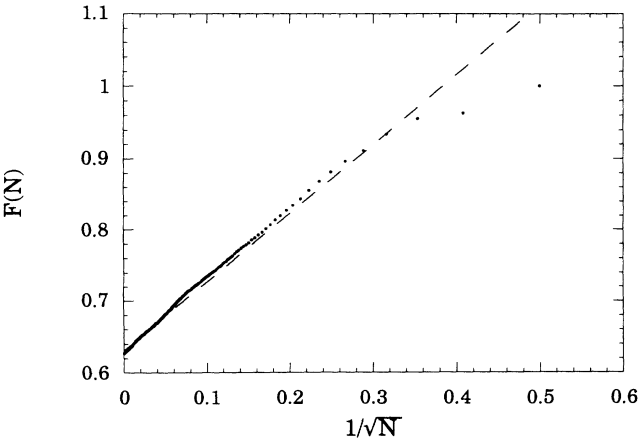

FIG. 8. The fraction $F(N)$ of symmetric walks which are longer than N steps as a function of $1/\sqrt{N}$. The data follow a linear relation of the type $F(N) \cong A + B/\sqrt{N}$. A least-squares linear fit of the data points for $N \geq 12$ (dashed line) gives $A = 0.628 \pm 0.001$ and $B = 1.04 \pm 0.01$.

that has come to equilibrium at a certain temperature. We then use this correspondence to argue that the fractal dimension of the symmetric tricolor walk is exactly 2 and that $\tau_3 = \frac{5}{2}$.

Let us first define the equilibrium SASAL. Let C be an arbitrary self-avoiding loop (SAL) of N bonds on the WS lattice. In order to assign an energy to this SAL, we walk around it, coloring the adjacent sites in the original lattice as we go. We first choose a bond in C, and let the label of the bond be (S_1^0, S_2^0, S_3^0). The sites S_1^0, S_2^0, and S_3^0 are colored black, white, and gray, respectively. Next, we traverse the bond in one of the two possible directions. The site just reached is shared by the WS cells centered on sites S_1^0, S_2^0, and S_3^0. It also belongs to a fourth WS cell centered on a site which we label S_4^0. Site S_4^0 is now colored in such a way that the next bond in the SAL is a tricord bond. We continue coloring in this fashion as we follow the SAL. To see what happens in the general case, consider the situation after the coloring of the sites adjacent to the bond (S_1, S_2, S_3) has just been completed. The site just reached is shared by the three WS cells centered on sites S_1, S_2, and S_3. It also belongs to a fourth WS cell centered on a site we will label S_4. We now color S_4 in such a way that the next bond in the SAL is a tricord bond. If S_4 has been colored previously, it is recolored. This recoloring can either change the color of S_4 or leave it unmodified. This process continues until we return to the point of departure.

We are now ready to assign an energy to the SAL. If the color of a site is changed at any point in the coloring process, the SAL has infinite energy—in other words, the conformation is forbidden. Otherwise, the energy of the loop is taken to be $\varepsilon s(C)$, where $s(C)$ is the number of bcc lattice sites adjacent to the loop. Thus each colored site is assigned an energy ε. Note that the number of times the sites are recolored, $n(C)$, is equal to $N+3-s(C)$. As it ought to be, the energy assigned to the SAL is independent of the bond chosen as the starting point for the coloring process, and of the direction we travel around the SAL. The energy is also unaffected by permutations of the colors assigned to the sites S_1^0, S_2^0, and S_3^0.

The partition function of the SAL at temperature T is

$$Z_N(T) = \sum_{C'} \exp[-\beta \varepsilon s(C')] , \tag{3.4}$$

where the sum runs over all allowed SAL configurations C' and $\beta \equiv T^{-1}$. The Boltzmann weight of a particular allowed configuration C is

$$w(C,N,T) = \exp[-\beta \varepsilon s(C)]/Z_N(T) . \tag{3.5}$$

The SAL we have defined has a certain set of forbidden configurations. It also has an attractive short-ranged interaction between monomers on sites in the same WS cell. This interaction has strength ε, and leads to higher Boltzmann weights for loop conformations with small numbers of adjacent sites. We expect this problem to be in the same universality class as the usual self-attracting SAW with NN interactions alone. If this is so, the SAL will have a mean radius of gyration $\langle R \rangle$ which scales as

N^{ν} at high temperatures, and the value of ν will be the same as that observed for the unconstrained 3D SAW in the absence of attractive monomer-monomer interactions [1]. Monte Carlo simulations of the latter problem have yielded the estimate $\nu_{\rm SAW}=D_{\rm SAW}^{-1}=0.592\pm0.003$ [34]. As the temperature is reduced, a collapse transition occurs at some temperature $T=T_{\Theta}$ with $T_{\Theta}/\varepsilon=O(1)$ [1]. For temperatures $T<T_{\Theta}$, the SAL has a nonzero density and ν assumes the value $\frac{1}{3}$. Finally, at the collapse transition temperature the value of ν is expected to be $\frac{1}{2}$, since the upper critical dimension for the Θ point is 3 [1,35].

We next consider the tricolor walk with $p=q=\frac{1}{3}$. Each new step the walk makes is a tricord bond. The probability that a particular step is made is $\frac{1}{3}$ if the target site is uncolored, and is 1 if the target site has already been colored. Any move which would necessitate a change in the color of the target site is forbidden, and so each time that a previously colored site is targeted, the next move is forced. The probability that a loop of length N is formed is

$$P(N)=\sum_{C'} 3^{-N}\exp[(\ln 3)n(C')] , \tag{3.6}$$

where the sum runs over all allowed SAL configurations of length N and $n(C')$ is the number of times that forced moves are made in the walk C'. The probability of a particular allowed loop configuration C (given that the walk closes in N steps) is

$$p(C,N)=P(N)^{-1}3^{-N}\exp[(\ln 3)n(C)] . \tag{3.7}$$

Let $T_0\equiv\varepsilon/\ln 3$. Comparing Eqs. (3.4) and (3.6) and using the relation $n(C)=N+3-s(C)$, we see that

$$Z_N(T_0)=\tfrac{1}{27}P(N) , \tag{3.8}$$

while from Eqs. (3.5) and (3.7) we obtain

$$w(C,N,T_0)=p(C,N) . \tag{3.9}$$

Equations (3.8) and (3.9) show that the SASAL at temperature $T=T_0$ is equivalent to the tricolor walk with $p=q=\frac{1}{3}$. In particular, Eq. (3.9) establishes that the loops in these two models have the same fractal dimension. The fractal dimension of the tricolor walk at its critical point can therefore assume only one of three possible values: 2, 3, or $D_{\rm SAW}$. On the basis of our Monte Carlo simulations, we can eliminate the latter two values and so conclude that the fractal dimension of the symmetric tricolor walk is exactly 2. It is interesting to note that it has been speculated that $d=3$ is the upper critical dimension of the SKW [5,9].

Although the equivalence we have established is exact, our argument that $D_3=2$ is not rigorous for several reasons. First of all, we cannot be certain that our self-attracting SAL is in the same universality class as the usual self-attracting SAW in 3D. Joining the ends of a SAW to form a SAL does not alter the value of ν in the high- or low-temperature phases or at the Θ point. However, the attractive interactions are longer ranged in our SAL than in the usual self-attracting SAW, and this may mean that the two collapse transitions are different universality classes. Indeed, the effect of NNN interactions on the 2D collapse transition has been debated at length [36]. The constraints on our SAL configurations may also alter the universality class. Finally, even if it is granted that the constrained, self-attracting SAL is in the same universality class as the self-attracting SAW with NN interactions alone, it is possible that a slow crossover occurs in the symmetric tricolor walk, and that the true asymptotic value of the fractal dimension is either 3 or $D_{\rm SAW}$. This scenario strikes us as unlikely, however, since we see no evidence for such a crossover in our simulations. Moreover, it has been established rigorously that the SKW on the hexagonal lattice is critical at $p=\frac{1}{2}$ [4], and the tricolor walk is expected to be critical at the point $p=q=\frac{1}{3}$ by analogy.

If we are correct in identifying $p=q=\frac{1}{3}$ as a critical point of the tricolor walk, then $T_0=\varepsilon/\ln 3$ is the *exact* collapse transition temperature of the SASAL. As far as we can determine, this is the first collapse transition temperature to be found exactly in 3D. This result should be quite useful in Monte Carlo studies of the collapse transition, since critical exponents can be computed much more precisely when the exact transition temperature is known.

Our mapping also enables us to find the exact value of τ_3. We have $Z_N(T_0)\sim\mu(T_0)^N N^{\alpha-2}$ for $N\gg 1$ [1]. Since $d=3$ is the upper critical dimension for the SASAL, the critical exponent α takes on the mean-field value $\frac{1}{2}$ [1]. Equation (3.8) now shows that τ_3 is exactly $\frac{5}{2}$, and that $\mu(T_0)$ must be 1. Our result $\tau_3=\frac{5}{2}$ is subject to the same caveats as our earlier result $D_3=2$. It is, however, in excellent agreement with our Monte Carlo value, $\tau_3=2.49\pm0.01$.

IV. ASYMMETRIC TRICOLOR WALKS

Let us consider trichromatic site percolation on the bcc lattice once again. The tricord bonds reside on edges of the WS lattice. We will say that a bond of the WS lattice is "occupied" if it is a tricord bond. The fraction of occupied bonds in the WS lattice is $f\equiv 6pqr$. The occupancy of the bonds in the WS lattice is correlated, since each site in the WS lattice belongs to either zero or two tricord bonds. For simplicity, let us confine our attention to the case $p=q$, so that $f=6p^2(1-2p)$. For small values of p, only finite loops will exist, but as p is increased, the average size of the loops grows. As we shall see, at a critical value of p which we denote by p_1, the average loop size diverges, and an infinite loop is formed. The critical value p_1 is less than $\frac{1}{3}$. When p exceeds $\frac{1}{3}$, f begins to decrease. A second percolation threshold occurs when a critical value p_2 is reached and for $p>p_2$, there are no infinite tricords. Since the correlations between bonds extend over short distances, we might be tempted to argue on the basis of universality that the percolation transitions at $p=p_1$ and $p=p_2$ should have the same critical exponents as uncorrelated bond percolation in 3D. We will see later that this is only partially true.

As stated in the preceding paragraph, we will focus our

attention on the line $p=q$ in the plane $p+q+r=1$. Monte Carlo simulations were performed for more than 40 different values of p in the range $[0.12, \frac{1}{3}]$. In each case, a walk was terminated if it reached the length $N_{\max}=2^{20}$. For $p \leq 0.255$, a total of 5000 walks were constructed for each value of p considered, while this number was increased to 20 000 for $0.255 < p \leq 0.288$ and to 10 000 for $p > 0.288$.

At the critical point $p=p_1$, we expect that $F(N) \sim N^{-\tau'+2}$ for large N, since the probability that a walk grows indefinitely vanishes for $p \leq p_1$. Figure 9 is a log-log plot of F as a function of N for three values of p. The data for $p=0.2915$ are fit well by a power law, while the corresponding plots for $p=0.291$ and 0.292 are curved for large N. We thus obtain the estimate $p_1=0.2915\pm0.0005$ for the critical point. Note that $p_1 > p_c$, and so there is a range of p values in which an infinite cluster of each of the three colors exists, but no infinite tricord occurs.

To estimate the critical exponent τ', a linear fit to the curve for $p=0.2915$ was performed for $N > 100$. This gives $\tau'=2.1804\pm0.0003$. The error quoted here is purely statistical in origin. By performing least-squares fits of our data for $p=0.291$ and $p=0.292$, we found that the main source of error in our value of τ' is the uncertainty in p_1. Our final estimate is $\tau'=2.18\pm0.01$, a value which is comparable to the most recent Monte Carlo estimate of the exponent τ for percolation in 3D, $\tau=2.186\pm0.008$ [37,38]. This result supports the idea that the critical exponents for the transition at $p=p_1$ are the same as for uncorrelated bond percolation in 3D.

In Fig. 10, we have plotted $\ln F(N)$ versus N for a range of p values. It appears that $F(N)$ decays exponentially to zero for $p < p_1$, and that $F(N)$ asymptotes to a nonzero constant for $p_1 < p < \frac{1}{3}$. Thus, as discussed at the beginning of this section, infinite walks exist for $p_1 \leq p \leq \frac{1}{3}$, but not for $p < p_1$.

We next computed the mean length N_i and the mean radius of gyration R_i of the closed walks in the ith bin at $p=p_1$. We used the same binning procedure as for the symmetric walk. A plot of $\log_2 R_i$ versus $\log_2 N_i$ is

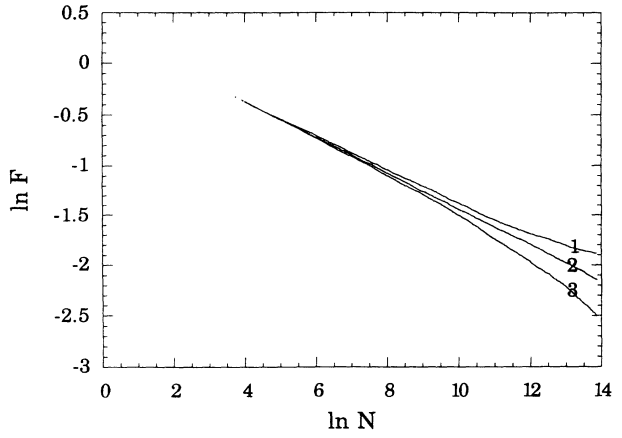

FIG. 9. Log-log plot of $F(N)$ as a function of N for $p=q=0.292$ (curve 1), 0.2915 (curve 2), and 0.291 (curve 3).

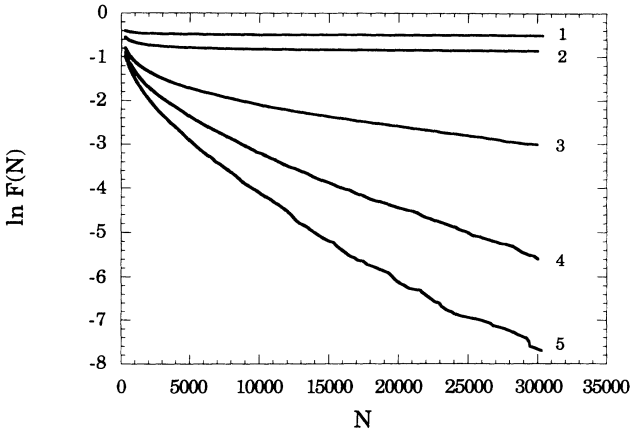

FIG. 10. Plot of $\ln F(N)$ vs N for $p=0.320$ (curve 1), 0.300 (curve 2), 0.285 (curve 3), 0.280 (curve 4), and 0.277 (curve 5).

curved, and so a finite-size analysis is needed to obtain an accurate estimate of the fractal dimension of the walks at threshold, D'. We therefore define the finite-size estimator

$$D_i' \equiv \frac{\log_2(N_{i+4}/N_{i-4})}{\log_2(R_{i+4}/R_{i-4})} . \tag{4.1}$$

In Fig. 11, our results for D_i' are plotted as a function of $1/R_i$. The data are well fit by a straight line, and extrapolation to the limit $R_i \to \infty$ gives $D'=2.54\pm0.01$. The Monte Carlo simulations of Ziff and Stell [37] yielded the estimate $D=2.529\pm0.016$ for the fractal dimension of 3D percolation clusters at threshold, and this value is consistent with earlier estimates [38]. Thus our result suggests that D and D' are in fact equal.

The exponents τ and D for percolation in 3D are related by the scaling relation $\tau=1+3/D$ [39]. The derivation of this relation is readily adapted to tricords in trichromatic site percolation, and we obtain $\tau'=1+3/D'$. Our estimates of τ' and D' are in good agreement with

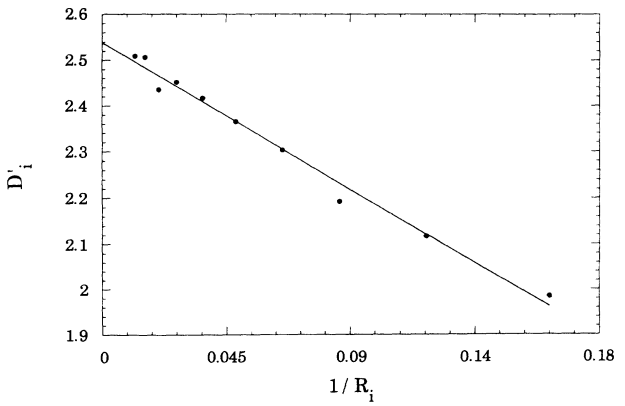

FIG. 11. The finite-size estimator D_i' for the fractal dimension of the walks at $p=p_1=0.2915$ plotted vs the inverse of the mean radius of gyration of the walks in the ith bin, R_i. A linear least-squares fit (solid line) was used to extrapolate the data to $1/R_i=0$, and gives $D'=2.54\pm0.01$.

this scaling relation.

For $p < p_1$, we expect the average walk length $\chi \equiv \sum_{N=1}^{\infty} NP(N)$ to diverge as $\chi \sim (p_1 - p)^{-\gamma'}$. To find an estimate for the exponent γ', we computed χ for a series of 36 values of p in the range [0.12, 0.286]. These values of p are denoted by p_j^*, where the subscript j is incremented from 1 to 36 as p is increased from 0.12 to 0.286. All the walks generated with p in this range closed before reaching the cutoff length $N_{\max}$, and so the value of χ was not affected by this limitation. A log-log plot of χ versus $(p_1 - p)$ is displayed in Fig. 12. A linear fit is inadequate because corrections to scaling play an important role in the range $p \in [0.12, 0.286]$. We assume these corrections have the form

$$\chi(p) \sim (p_1 - p)^{-\gamma'} [1 + A(p_1 - p) + B(p_1 - p)^{\delta} + \cdots] , \tag{4.2}$$

and we define the estimator

$$\gamma'_j \equiv \frac{\ln[\chi(p^*_{j-4})/\chi(p^*_{j+4})]}{\ln[(p_1 - p^*_{j+4})/(p_1 - p^*_{j-4})]} . \tag{4.3}$$

According to these relations, for $p_1 - p_j^* \ll 1$ we have

$$\gamma'_j \cong \gamma' - A(p_1 - p_j^*) - \delta B(p_1 - p_j^*)^{\delta} + \cdots \tag{4.4}$$

if $0 < \delta \leq 2$. The estimator γ'_j is plotted as a function of $(p_1 - p_j^*)$ in Fig. 13. The data points are well fit by a straight line, indicating that $\delta > 1$. Extrapolation to the limit $p = p_1$ gives $\gamma' = 2.02 \pm 0.01$. This value is very different from that found for the percolation transition in 3D [37,38], $\gamma = 1.795 \pm 0.005$, and definitely refutes the intuitive notion that all the exponents are the same.

For $p < p_1$, we expect $P(N)$ to have the scaling form [30]

$$P(N) = N^{1-\tau'} g((p_1 - p)N^{\sigma'}) , \tag{4.5}$$

where $g(x)$ is a scaling function which tends to a positive constant as $x \to 0$ and which decays exponentially to zero as $x \to \infty$. Inserting this form in the definition of χ, we

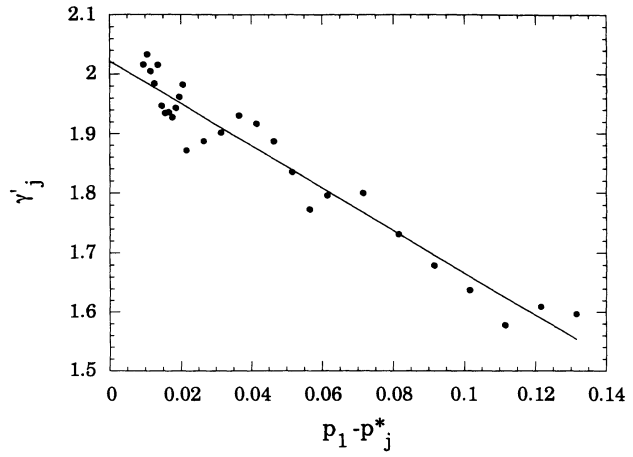

FIG. 13. The estimator γ'_j for the critical exponent γ' as a function of $(p_1 - p_j^*)$. Linear extrapolation of the data to $p = p_1$ (solid line) yields $\gamma' = 2.02 \pm 0.01$.

obtain the scaling relation

$$\gamma' = \frac{3 - \tau'}{\sigma'} \tag{4.6}$$

which, together with our estimates of γ' and τ', yields $\sigma' = 0.406 \pm 0.004$. Equation (4.5) gives the following scaling form for P_i:

$$P_i = N_i^{1-\tau'} h((p_1 - p)N_i^{\sigma'}) , \tag{4.7}$$

where h is a scaling function. To test this scaling form, we plotted $P_i N_i^{\tau'-1}$ versus $(p_1 - p)N_i^{\sigma'}$ for several values of p in the range [0.240,0.291] (Fig. 14). The reasonable collapse of the data confirms the scaling form (4.7) and shows that our estimates for γ' and τ' are consistent.

So far, we have ignored the segment $p_1 < p < \frac{1}{3}$ of the line $p = q$. To investigate the behavior of the tricolor walk in this region, we first reproduced the analysis of Sec. III A for the open walks. The average squared dis-

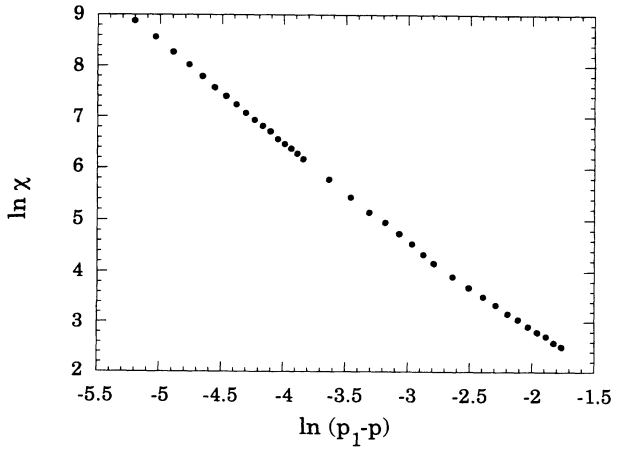

FIG. 12. Log-log plot of the average length χ of the closed walks as a function of $(p_1 - p)$.

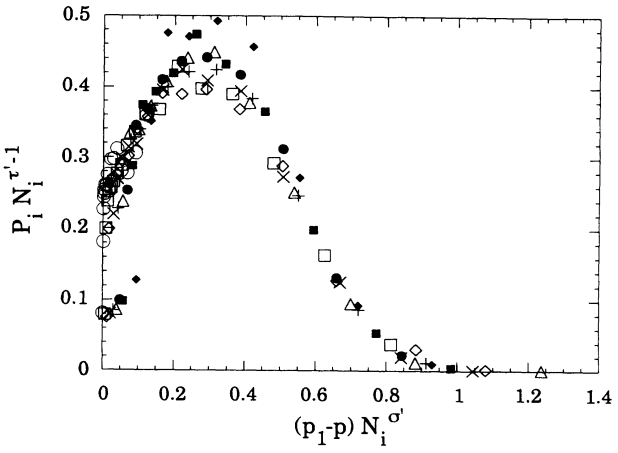

FIG. 14. Plot of $P_i N_i^{\tau'-1}$ vs $(p_1 - p)N_i^{\sigma'}$ for $p = 0.240$ (♦), 0.260 (■), 0.265 (●), 0.270 (△), 0.275 (+), 0.280 (×), 0.285 (◇), 0.288 (□), and 0.291 (○).

tance $\langle R^2(\Delta)\rangle$ between pairs of sites Δ steps apart was calculated and used to compute the estimator $D_e(\Delta)$ for the fractal dimension. In Fig. 15, $D_e(\Delta)$ is plotted as a function of $\log_2(\Delta)$ for several values of p in the range $[0.2915,\frac{1}{3}]$. Since some of the open walks were about to close when the cutoff length $N_{\max}$ was reached, the measured value of $\langle R^2(\Delta)\rangle$ becomes progressively smaller than the true value as Δ approaches $N_{\max}$. As a consequence, $D_e(\Delta)$ is systematically overestimated for the largest Δ values. This effect is more marked for $p=p_1$ than for $p>p_1$ because no error is incurred for infinite walks, and infinite walks occur only for $p>p_1$. For $p=0.300$, 0.310, and 0.320, we observe a crossover towards an apparent asymptotic fractal dimension of 2. This crossover is longer but qualitatively similar to that observed for $p=\frac{1}{3}$. It therefore seems likely that for all p in the interval $I\equiv(p_1,\frac{1}{3}]$, the fractal dimension D_3 asymptotically crosses over to a value of 2. Finally, $D_e(\Delta)$ appears to saturate at a value slightly higher than 2.5 when $p=p_1=0.2915$, in agreement with the value found previously, $D'=2.54\pm0.01$.

We next computed the average length of the walks of length N_0 or less, $L(N_0)\equiv\sum_{N=1}^{N_0}NP(N)$, for $p\in I$. For $p=\frac{1}{3}$, we know that $P(N)\sim N^{1-\tau_3}$, and τ_3 is believed to be exactly equal to $\frac{5}{2}$. Thus

$$L(N_0)\sim(N_0)^{1/2} \tag{4.8}$$

for $p=\frac{1}{3}$ and $N_0\gg1$. Since we have numerical evidence that the fractal dimension is 2 throughout the interval I, it seems likely that τ_3 is also constant in this region. Let us suppose that this is in fact the case. Equation (4.8) is then valid for any $p\in I$. Figure 16 is a plot of $L(N_0)$ as a function of $(N_0)^{1/2}$ for $p=0.3$, 0.31, and $\frac{1}{3}$. Equation (4.8) seems to apply in each case, which confirms our supposition that $\tau_3=\frac{5}{2}$ for all $p\in I$ [40]. We conclude that $\chi=\lim_{N_0\to\infty}L(N_0)$ is infinite throughout the interval I.

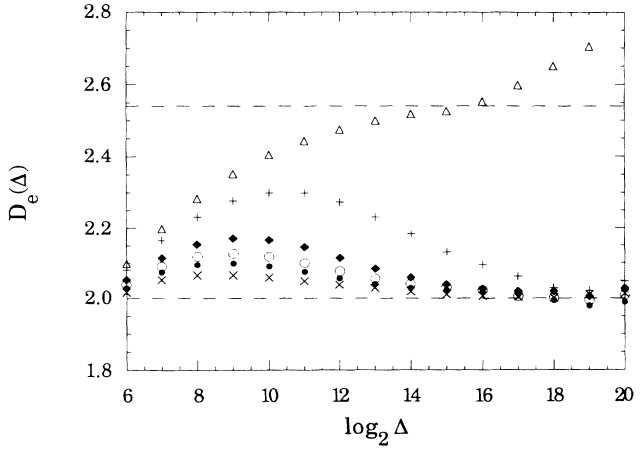

FIG. 15. The finite-size estimator $D_e(\Delta)$ for the fractal dimension of the open walks as a function of $\log_2\Delta$ for $p=q=\frac{1}{3}$ (×), 0.32 (●), 0.31 (◆), 0.30 (+), 0.2915 (△), and for $p=0.30$ and $q=0.34$(○).

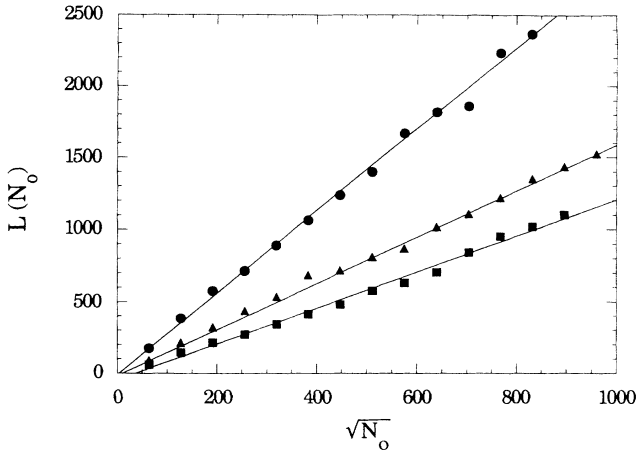

FIG. 16. The average length $L(N_0)$ of the walks of length N_0 or less plotted as a function of $(N_0)^{1/2}$ for $p=q=\frac{1}{3}$ (■), 0.31 (▲), and 0.30 (●). The solid lines are linear fits of the data points.

Our results also strongly suggest that the critical exponents D_3 and τ_3 are the same for $p_1<p\leq\frac{1}{3}$.

Up until this point, we have restricted our analysis to the line $p=q$ for the sake of simplicity, but we do not believe that this line is special in any respect. Instead, we expect that there is a line of critical points in the plane $p+q+r=1$ which encloses the point $p=q=\frac{1}{3}$. Everywhere inside this loop of critical points, the asymptotic behavior of the tricolor walk should be the same as at $p=q=\frac{1}{3}$. The critical behavior at each point on the loop itself should be the same as that observed for $p=q=p_1$. Finally, outside the loop the walks should always be finite. This picture is corroborated by additional simulations which were performed for $p=0.3$ and $q=0.34$. The estimator $D_e(\Delta)$ appears to cross over to the value 2 (Fig. 15), so that this point is expected to be inside the loop of critical points.

V. CONCLUSIONS

In this paper we introduced the tricolor walk, a growing SAW that is a direct generalization of the smart kinetic walk to 3D. Our growing walk is readily simulated, even though it is "smart". The tricolor walk directly constructs a tricord hull for polychromatic percolation with three colors, black, white, and gray. The tricolor walk depends on two parameters, p and q, which are the fraction of sites colored black and white, respectively.

In the symmetric tricolor walk, all allowed moves for the walker are equally weighted and $p=q=\frac{1}{3}$. Our Monte Carlo simulations strongly suggest that the fractal dimension of the symmetric tricolor walk is 2. We demonstrated that the symmetric tricolor walk is equivalent to a self-attracting SAW that has come to equilibrium at a certain temperature T_0. This equivalence was then used to argue that T_0 must be the Θ temperature for the self-attracting SAW, and hence that the fractal dimension of the symmetric walks is exactly 2.

As in the case of the SKW on the 2D hexagonal lattice, the tricolor walk is intimately related to percolation and to Θ polymers. The tricolor walk directly generates tricords for trichromatic percolation, and so facilitates numerical studies of tricords. It also permits us to construct very long polymer chains at their Θ point. This may prove useful in resolving a dispute concerning the corrections to scaling at the Θ point in 3D [41].

Asymmetric tricolor walks with $p=q<\frac{1}{3}$ undergo a percolation transition at $p=p_1=0.2915\pm0.0005$: there are infinite walks for $p_1\leq p\leq\frac{1}{3}$, but not for $p<p_1$. The fractal dimension of the walks at threshold, $D'=2.54\pm0.01$, is close to the fractal dimension of bulk percolation clusters at threshold in regular 3D percolation. In contrast, the mean length of the finite walks χ diverges as $(p_1-p)^{-\gamma'}$ as the threshold is approached from below, and our estimate $\gamma'=2.02\pm0.01$ differs markedly from the exponent γ for regular percolation in 3D. We also found that χ is divergent for $p_1<p\leq\frac{1}{3}$, whereas in regular percolation χ is finite for all values of p except the threshold value p_c.

Our Monte Carlo simulations indicate that the percolation transition that occurs in the tricolor walk is in a different universality class than the usual percolation transition in 3D. We believe that this is because tricords are topologically linear, i.e., they are closed loops of occupied bonds. Topological constraints have been shown to be relevant in other critical phenomena [7,8,42,43]. For example, lattice animals that are topologically linear are in a different universality class than unrestricted lattice animals [42]. Perhaps our most intriguing finding is that some critical exponents are affected by the linearity constraint, while others are not. A full understanding of these observations must await future work.

ACKNOWLEDGMENTS

We are grateful to B. Berche for helpful discussions. One of us (J.-M.D.) wishes to thank NATO for a research grant. R.M.B. was supported by a grant from the IBM Corporation and by NSF Grant No. DMR-9100257.

*Permanent address: Laboratoire de Physique du Solide, Université de Nancy I, F-54506 Vandoeuvre-lès-Nancy, France.

[1] For example, see P. G. de Gennes, *Scaling Concepts in Polymer Physics* (Cornell University Press, Ithaca, 1979).
[2] D. J. Amit, G. Parisi, and L. Peliti, Phys. Rev. B **27**, 1635 (1983).
[3] I. Majid, N. Jan, A. Coniglio, and H. E. Stanley, Phys. Rev. Lett. **52**, 1257 (1984); J. W. Lyklema and K. Kremer, J. Phys. A **17**, L691 (1984); **19**, 279 (1986); S. Hemmer and P. C. Hemmer, J. Chem. Phys. **81**, 584 (1984).
[4] A. Weinrib and S. A. Trugman, Phys. Rev. B **31**, 2993 (1985).
[5] K. Kremer and J. W. Lyklema, Phys. Rev. Lett. **54**, 267 (1985).
[6] K. Kremer and J. W. Lyklema, J. Phys. A **18**, 1515 (1985).
[7] R. M. Bradley and D. Kung, Phys. Rev. A **34**, 723 (1986).
[8] J.-M. Debierre and L. Turban, J. Phys. A **19**, L131 (1986).
[9] J. W. Lyklema, C. Evertsz, and L.Pietronero, Europhys. Lett. **2**, 77 (1986).
[10] P. Meakin, Phys. Rev. A **37**, 2644 (1988).
[11] H. Saleur and B. Duplantier, Phys. Rev. Lett. **58**, 2325 (1987).
[12] A closely related model is considered in Ref. [9]. See also J. W. Lyklema and C. Evertsz, J. Phys. A **19** L895 (1986); G. F. Lawler, Duke Math. J. **47**, 655 (1980); G. F. Lawler, J. Phys. A **20**, 4565 (1987).
[13] A comparable result was obtained in the more extensive simulations reported later in Ref. [10].
[14] B. Nienhuis, Phys. Rev. Lett. **49**, 1062 (1982).
[15] L. Peliti, J. Phys. (Paris) Lett. **45**, L925 (1984); L. Pietronero, Phys. Rev. Lett. **55**, 2025 (1985); K. Kremer and J. W. Lyklema, *ibid.* **55**, 2091 (1985).
[16] J. W. Lyklema, J. Phys. A **18**, L617 (1985).
[17] For a review of hull-generating walks, see R. M. Ziff, Physica D **38**, 377 (1989).
[18] A. Coniglio, N. Jan, I. Majid, and H. E. Stanley, Phys. Rev. B **35**, 3617 (1987).
[19] B. Duplantier and H. Saleur, Phys. Rev. Lett. **59**, 539 (1987).
[20] (a) R. M. Bradley, Phys. Rev. A **39**, 3738 (1989); (b) **41**, 914 (1990).
[21] P. N. Strenski, R. M. Bradley, and J.-M. Debierre, Phys. Rev. Lett. **66**, 1330 (1991).
[22] R. M. Bradley, P. N. Strenski, and J.-M. Debierre, Phys. Rev. B **44**, 76 (1991).
[23] R. Zallen, Phys. Rev. B **16**, 1426 (1977).
[24] J. W. Halley, in *Percolation Structures and Processes*, edited by G. Deutscher, R. Zallen, and J. Adler, *Annals of the Israel Physical Society* (Hilger, Bristol, 1983), Vol. 5
[25] J. W. Halley and W. K. Holcomb, Phys. Rev. Lett. **40**, 1670 (1978).
[26] J. W. Halley, W. K. Holcomb, and K. Goetz, Phys. Rev. B **21**, 4840 (1980).
[27] F. Scholl and K. Binder, Z. Phys. B **39**, 239 (1980).
[28] T. Grossman and A. Aharaony, J. Phys. A **19**, L745 (1986); **20**, L1193 (1987); S. S. Manna, *ibid.* **22**, 433 (1988).
[29] A bond in the WS lattice of the simple cubic lattice belongs to four different WS cells. A bond is considered to be an element of a tricord if each of the three colors appears at the center of one of these WS cells.
[30] R. M. Ziff, Phys. Rev. Lett. **56**, 545 (1986).
[31] Unfortunately, the data for the closed loops are too noisy to permit a meaningful finite-size analysis.
[32] R. M. Ziff, E. G. D. Cohen, and X. P. Kong, Phys. Rev. A **44**, 2410 (1991).
[33] W. Feller, *Introduction to Probability Theory and Its Applications* (Wiley, New York, 1966), Vol. 2, p. 579.
[34] N. Madras and A. D. Sokal, J. Stat. Phys. **50**, 109 (1988).
[35] P. G. de Gennes, J. Phys. (Paris) Lett. **36**, L55 (1975).
[36] See Ref. [20(b)], and references therein.
[37] R. M. Ziff and G. Stell (unpublished).
[38] Numerical estimates of the critical exponents for percolation are reviewed in J. Adler, Y. Meir, A. Aharony, and A. B. Harris, Phys. Rev. B **41**, 9183 (1990).
[39] D. Stauffer, *Introduction to Percolation Theory* (Taylor and

Francis, London, 1985).
[40] The data for $p=0.32$ also appear to follow Eq. (4.8), but were omitted from Fig. 16 for the sake of clarity.
[41] B. Duplantier, J. Phys. (Paris) **43**, 991 (1982); A. L. Kholodenko and K. F. Freed, J. Chem. Phys. **80**, 900 (1984); J. Phys. A **17**, L191 (1984); B. Duplantier, Europhys. Lett. **1**, 491 (1986); J. Chem. Phys. **86**, 4233 (1987).
[42] D. S. Gaunt, A. J. Guttman, and S. G. Whittington, J. Phys. A **12**, 75 (1979); F. Family, *ibid.* **13**, L325 (1980).
[43] J.-M. Debierre and R. M. Bradley, J. Phys. A **22**, L213 (1989).

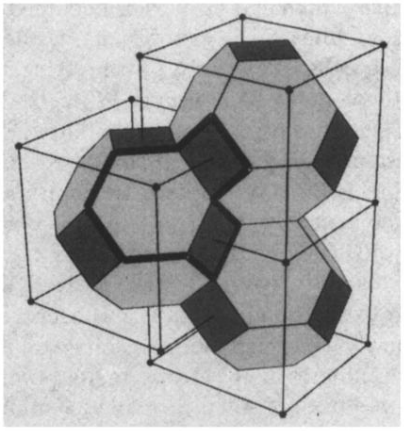

FIG. 2. Wigner-Seitz lattice for the bcc lattice. The sites of the bcc lattice (solid circles) form two interpenetrating simple cubic lattices. The Wigner-Seitz lattice is a space-filling packing of truncated octahedra (shaded solids). A site of the bcc lattice resides at the center of each truncated octahedron. An example of a SKW that cannot be generated by the tricolor walk is shown using bold lines.